NJC

PAPER

View Article Online
View Journal | View Issue

Cite this: *New J. Chem.*, 2014, **38**, 1965

Amphiphilic iron(II) complexes with short alkyl chains – crystal packing and spin transition properties†

Stephan Schlamp, Katja Dankhoff and Birgit Weber*

Received (in Victoria, Australia) 23rd August 2013,
Accepted 15th October 2013

DOI: 10.1039/c3nj00991b

www.rsc.org/njc

An amphiphilic iron(II) spin crossover complex with relatively short octyl chains was synthesised and the crystal structures of the high spin and the low spin state could be determined. In further reactions, a second modification of the hexa-coordinated complex and two different penta-coordinated complexes could be obtained and characterised by X-ray structure analysis. The examples demonstrate an influence of the alkyl chains on the stoichiometry of the final product. Different arrangements of the alkyl chains were observed in the crystal packing. Despite those differences, the spin transition of the hexa-coordinated complexes is always gradual and comparable to that observed in solution.

Introduction

Since the discovery of the spin crossover (SCO) phenomenon in 1931,[1] a vast amount of compounds showing spin transition with a huge variety of ligands and metal centres have been synthesised.[2,3] In recent times, the interest in adding multi-functionality to these compounds has increased so that they exhibit not only spin crossover but also additional functionalities like liquid crystallinity,[4] gel formation[5] or magnetic exchange interactions,[6] just to mention three examples. Also the nano-structuring of spin crossover compounds, either by the synthesis of nanoparticles[7] or through patterning methods,[8] is a recent field of research that is an important step towards possible future applications.

For cooperative SCO materials intermolecular interactions like hydrogen bonds, π–π interactions or also van der Waals (vdW) interactions are of utmost importance. Studies on compounds exhibiting huge hysteresis showed that particularly hydrogen bonds are related to strong cooperative effects leading to the hysteresis phenomenon.[9] This work is focused on the influence of vdW interactions on the spin crossover behaviour. The addition of long alkyl chains to the periphery of the ligand adds a new functionality to the spin crossover system by the generation of amphiphilic molecules.[10] In previous work we did show that such complexes with Schiff base-like ligands can self-assemble into lipid layer like arrangements.[11,12] Additionally, an influence of the alkyl chains on the spin transition behaviour is possible. A rearrangement of the alkyl chains could trigger the spin transition or *vice versa*.[13] Thus the modification of the ligand could help to increase the cooperativity of spin crossover complexes based on the Schiff base-like ligand system used in our group. In a crystal engineering approach we want to study the influence of these alkyloxy substituents as a structure determining element on the packing of the complexes in the crystal and therefore on the SCO behaviour. So far, lipid layer like structures are the only motif observed for such complexes with dodecyl or hexadecyl alkyl chains.[11,12] Thus the question arises if other structural motifs are possible and to what extent the alkyl chains influence the crystal packing and by this the magnetic properties. Here we present X-ray structures and magnetic properties of complexes with comparatively short octyl chains.

Synthesis and general characterisation

The synthesis of the new amphiphilic ligand, visualised in Scheme 1, is realised in a four step reaction. In the ESI,† Fig. S1, the NMR spectrum of the free ligand **H_2L** is displayed with the signal assignment. Conversion with iron(II)-acetate[14] results in the hexa-coordinated complex [**Fe(L)(MeOH)$_2$**] with two methanol as axial ligands. Replacement of the methanol molecules with 4-dimethylaminopyridine (dmap) leads, depending on the exact reaction conditions, to the desired compound [Fe(L)(dmap)$_2$] (**1**) (with varying amounts of included methanol molecules) or the penta-coordinated complex [Fe(L)(dmap)] (**2**). In a first approach a 30-fold excess of dmap was used with the aim of

Inorganic Chemistry II, Universität Bayreuth, Universitätsstraße 30, NW 1, 95440 Bayreuth, Germany. E-mail: weber@uni-bayreuth.de; Fax: +49-92155-2157; Tel: +49-92155-2555

† Electronic supplementary information (ESI) available: ^{1}H NMR spectrum of H_2L, magnetic susceptibility data for the iron complexes discussed in the work and parameters used in the X-ray structure determination. CCDC 944434–944438. For ESI and crystallographic data in CIF or other electronic format see DOI: 10.1039/c3nj00991b

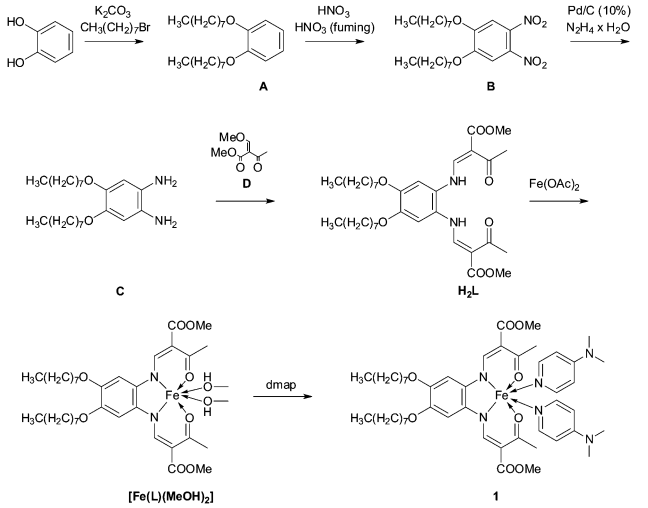

Scheme 1 General procedure for the synthesis of the new amphiphilic Schiff base-like ligand and its iron(II) complexes.

obtaining an octahedral complex. Indeed, the desired complex $[Fe(L)(dmap)_2]\cdot MeOH$ (**1a**) could be isolated. However, slight variations in the reaction conditions (reaction time, temperature of precipitation), keeping the stoichiometry constant, resulted in the isolation of the penta-coordinated complex [Fe(L)(dmap)] (**2**). Here two different samples (**2a** and **2b**), both with the same composition but differences in the relative orientation of the alkyl chains, were obtained. This was unexpected as the characteristic colour change of the solution upon cooling with liquid nitrogen suggested the presence of a hexa-coordinated species in solution. Due to the contrasting results further syntheses with a different excess of the axial ligand were carried out to obtain a clear synthetic protocol for the compounds **1** and **2**. The excess of the axial dmap ligand was systematically varied and stoichiometries of **1**: 20, 30, 50, 70, 90 and 110 were used. It turned out that the penta-coordinated product (**2**) was obtained selectively with a 20 fold excess. By taking 30 equivalents of the axial ligand, it is difficult to predict if the penta- or hexa-coordinated complex will be obtained. In our synthetic approaches a 50 : 50 ratio between the two possibilities was reached. But the system can be forced to precipitate hexa-coordinated when a 50 fold excess or higher is used. In this frame, another modification of the hexa-coordinated complex, **1b** ($[Fe(L)(dmap)_2]\cdot 1.5MeOH$), was obtained, that could be characterised by single crystal X-ray structure analysis. For the approaches with a higher excess of dmap, fine crystalline samples with additionally included dmap/MeOH molecules were obtained.

The compounds were characterised by elemental analysis, IR and mass spectrometry, magnetic measurements and, if possible, X-ray structure analysis.

Description of the X-ray structures

Single crystals suitable for X-ray structure analysis were obtained for two hexa-coordinated (**1a** and **1b**) and two penta-coordinated (**2a** and **2b**) samples. The quality of the data of **1b** was low (high R_{int}) thus only the conformation of the complex and the relative orientation of the molecules in the crystal packing can be presented. In the case of **2a** the disorder of the alkyl chains could not be solved satisfactorily (due to the low quality of the dataset and twinning of the crystal) thus only the conformation of the molecule is presented. Attempts to reproduce the crystals to obtain diffraction data of higher quality led to the sample **2b**. In the ESI,† Table S1, the crystallographic data are given.

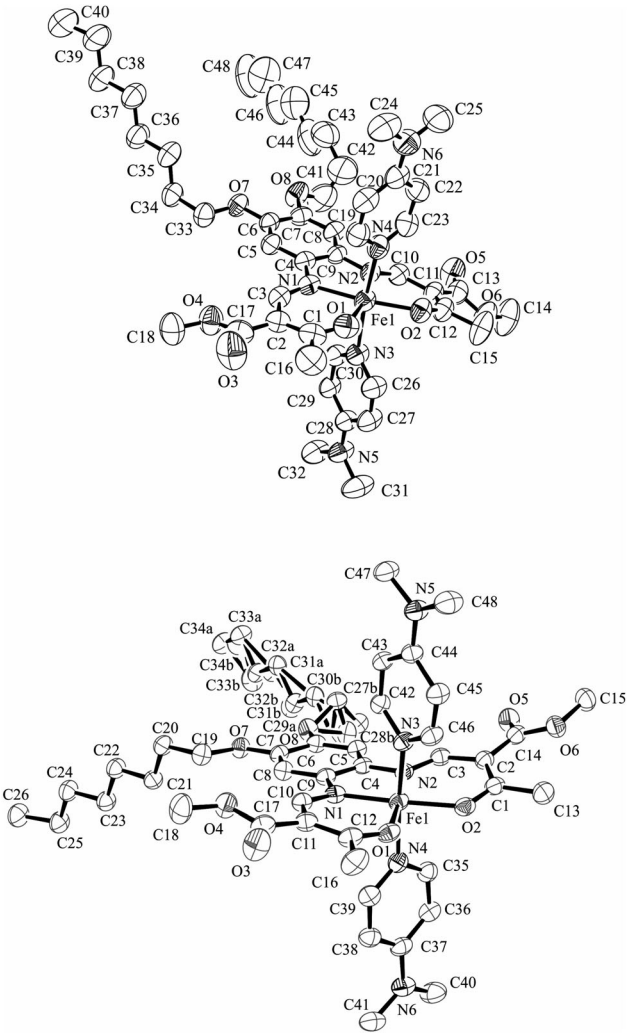

Fig. 1 ORTEP drawing of **1a** at 273 K (HS) (top) and 133 K (LS) (bottom). Ellipsoids are drawn at the 50% probability level. Hydrogen atoms and methanol molecules are omitted for clarity.

1a precipitated in the form of platelet-like crystals out of a black solution with a 30 fold excess of dmap. The crystal structure was determined at 273 K and 133 K, which correspond to the high spin (HS) and the low spin (LS) state of the system (see magnetic measurements). In Fig. 1 the asymmetric unit of **1a** in the HS and the LS state is displayed. Selected bond lengths and angles are summarised in Table 1.

1a crystallises in the triclinic space group $P\bar{1}$ that does not change upon spin transition. The bond lengths and angles within the first coordination sphere, $Fe–N_{eq}/Fe–O_{eq}$, have an average

Table 1 Selected bond lengths/Å and angles/° within the inner coordination sphere of **1a** (LS) and **1a** (HS), **1b**, **2a** and **2b**

	$Fe–N_{eq}$/Å	$Fe–O_{eq}$/Å	$Fe–N_{ax}$/Å	O–Fe–O/°
1a (LS)	1.909(2)/1.915(2)	1.948(1)/1.957(1)	2.013(2)/2.018(2)	91.68(6)
1a (HS)	2.065(3)/2.080(3)	2.002(3)/2.012(3)	2.216(3)/2.217(3)	107.16(11)
1b	1.9	2.0	2.0	92
2a	2.1	2.0	2.1	100
2b	2.073(4)/2.085(4)	2.002(3)/1.980(3)	2.127(4)	101.62(14)

of 2.07/2.01 Å (HS) and 1.91/1.95 Å (LS) in the region expected for this ligand system with a bond length change of about 5% upon spin transition.[15,18] The average Fe–N distances to the axially attached ligands (2.22 Å (HS) and 2.02 Å (LS)) change by about 10% (see Table 1) due to the higher flexibility of the axial ligands. The O–Fe–O angle is 91.7° (LS) and 107.2° (HS) in the expected region for complexes of this type of Schiff base-like ligands.[15,18] The change of the unit cell volume is $\Delta V/V = 4.0\%$ at the lower limit of what is expected for an iron(II) spin crossover complex,[3] but the value is higher than the one previously reported for an SCO complex with C16-alkyl chains.[12]

One of the alkyl chains and the methanol molecule are disordered in the LS state. Due to increase of thermal motion of the atoms at higher temperatures, this disorder cannot be solved in the HS state. The relative orientation of the aromatic planes of the dmap to each other changes marginally from 89.3° to 88.1°, and the N_{ax}–Fe–N_{ax} angle from 175.7° to 174.9° upon switching from the LS to the HS state, thus the axial ligands are nearly perpendicular in both spin states.

1b precipitated as spicular crystals, space group $P2_1/c$, from the synthetic approach with 50 fold excess of dmap and the X-ray structure was determined at 133 K. Due to insufficient quality of the data one can only talk about a motif. Average values of selected bond lengths and angles are summarised in Table 1.

Fig. 2 shows the asymmetric unit of **1b**. At the temperature used for the determination of the X-ray structure the complex

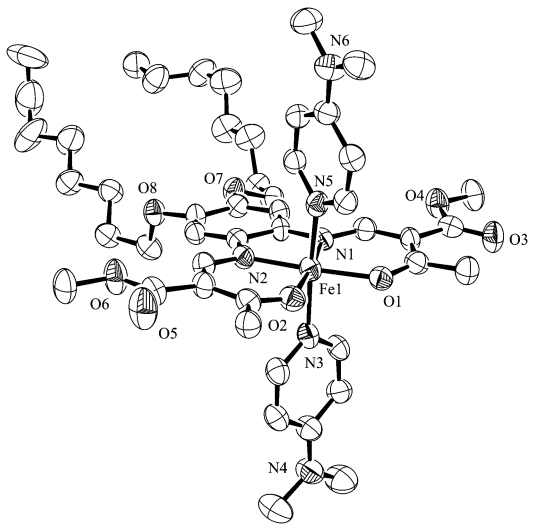

Fig. 2 ORTEP drawing of **1b**. Ellipsoids are shown at the 50% probability level. Hydrogen atoms and methanol molecules are omitted for clarity.

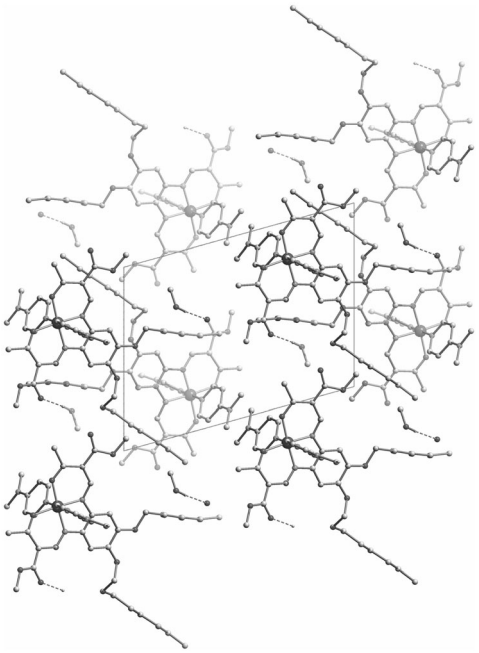

Fig. 3 Molecular packing of **1a** (LS) along [100]. Hydrogen bonds are drawn as dashed lines. Disorder omitted for clarity.

should be in the LS state according to the magnetic measurements. Indeed, the bond lengths and angles within the first coordination sphere are very similar to those of **1a** in the LS state. The average values are 1.9 Å/2.0 Å for $Fe–N_{eq}$/$Fe–O_{eq}$ and 2.0 Å for $Fe–N_{ax}$. The O–Fe–O angle is about 92°, the N_{ax}–Fe–N_{ax} angle is 174° and the dmap rings are twisted towards each other by an angle of around 94° and are therefore also nearly perpendicular. The main difference between the two samples lies in the additional half of the solvent molecule, the conformation (orientation of the alkyloxy chains) and the packing of the molecules in the crystal.

In the molecular packing of **1a**, displayed in Fig. 3 for the LS state, the disordered methanol molecule forms a hydrogen bond with the O5 atom in the outer periphery of the equatorial ligand. This hydrogen bond is weakened in the HS state. A few further short contacts (more than 0.2 Å shorter than the sum of the vdW radii) are observed, which are given in Table 2. The major distinction between the molecular packing of **1a** compared to the previously discussed structures is the absence of a lipid layer like structure. Instead, the axial dmap ligand of one complex is "embraced" from the C8 chains of the neighbouring complex. For the previously published structures the distance between the alkyl chains are between 0.3 and 0.4 Å longer than

Table 2 Short contacts and hydrogen bonds/Å and the corresponding angle/° of the obtained crystal structures

	D–H···A	D–H	H···A	D···A	D–H···A
1a (LS)	C47–H47B···O7[a]	0.98	2.60	3.436(3)	143
	C29A–H29B···C42[b]	0.97	2.637	3.519(8)	151
	C41–H41C···O2[c]	0.98	2.57	3.393(3)	142
	O31B–H31F···O5[d]	0.84	1.92	2.760(3)	174
1a (HS)	C32–H32B···C6[e]	0.96	2.606	3.550(6)	165
	O9A–H9A···O5[f]	0.82	2.04	2.785(14)	151
2b	C23–H23C···O4[g]	0.98	2.400	3.347(7)	162

[a] $1 + x, y, z$. [b] $1 - x, 1 - y, - z$. [c] $1 - x, 2 - y, 1 - z$. [d] x, y, z. [e] $1 + x, y, z$. [f] $1 - x, 1 - y, 1 - z$. [g] $-1 + x, y, z$.

the sum of the vdW radii, indicative of stabilising interactions between the chains.[11,12] For **1a** in the LS state several short contacts are observed between the alkyl chains, and the alkyl chains and the embraced dmap, respectively. However, the contacts are too short to be considered for a stabilising effect. In the HS state they are a bit longer. The strength of such stabilising interactions (London dispersion forces) depends on the length of the alkyl chains. Obviously, for the complex discussed here, the C8 alkyl chains are not long enough to form lipid layer like structures.

The packing of the molecules in the crystal of **1b** is very different to that of **1a** (Fig. 4). Two molecules form pairs where the alkyl chains are arranged such that stabilising vdW interactions can be considered. The next pair is rotated by 90° with the two axial dmap ligands pointing together. As only a structural motif is obtained, no intermolecular contacts can be discussed. It can, however, be pointed out that, as for **1a**, no lipid layer like arrangement of the complex molecules is obtained.

The two penta-coordinated complexes crystallise in the space group $P2_1/c$ (**2a**) and $P\bar{1}$ (**2b**), respectively. In Fig. 5 ORTEP drawings of the asymmetric units of **2a** and **2b** are displayed. In Table 1 selected bond lengths and angles within the first coordination sphere are given. For these two samples, no additional methanol molecules are included in the crystal packing.

Due to insufficient quality of the data of the spicular crystals of **2a**, only the conformation of the molecule is discussed in comparison to that of **2b**.

The average bond lengths of the inner coordination spheres of the two penta-coordinated species are about 2.1 Å ($Fe–N_{eq}$) and 2.0 Å ($Fe–O_{eq}$) very similar to the lengths of the HS structure of **1a** and in the same order of magnitude as observed for other penta-coordinated complexes of this ligand system.[16,17] The $Fe–N_{ax}$ bond lengths are about 0.1 Å shorter than in **1a** (HS), due to the penta-coordination. The O–Fe–O angles are 100° in the region expected for complexes with this kind of Schiff base-like ligands and are between the values of the HS and the LS state, respectively.[16,17]

In the case of **2a** the C8 alkyl chains are spread widely out with an angle of almost 90° between the two chains. In contrast to this, for **2b** they are arranged parallel to each other, similar to **1b**. However, differently to **1b**, in **2b** the alkyl chains are not in plane with the axial ligand but bent by almost 90° in the direction of the axial dmap ligand.

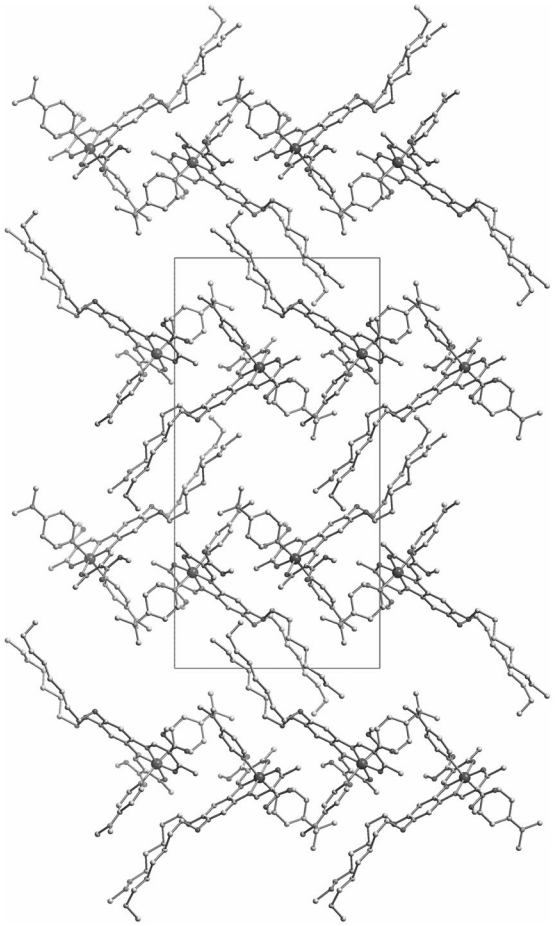

Fig. 4 Molecular packing of **1b** along [100]. Methanol molecules are omitted for clarity.

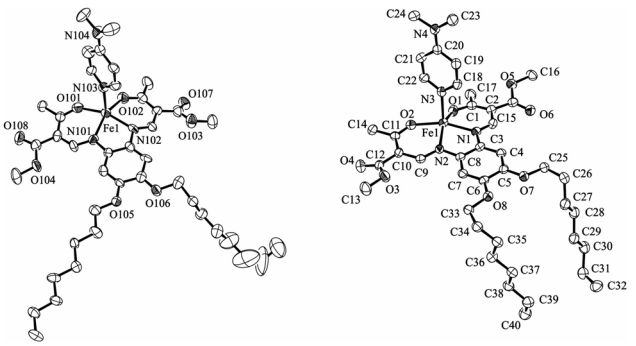

Fig. 5 ORTEP drawing of **2a** (left) and **2b** (right). Ellipsoids are shown at the 50% probability level. Hydrogen atoms are omitted for clarity.

In Fig. 6 the molecular packing in the unit cell of **2b** is displayed. In this case, pairs are built where the almost planar planes of the equatorial ligand including the iron(II) (the iron-N1N2O1O2 plane distance is 0.36 Å) are stacked above each other and the C8 alkyl chains are bent in the direction of the axial dmap of the neighbouring molecule. A short contact with a distance of 0.2 Å smaller than the sum of the vdW radii connects one molecule at the atom H23C of the dmap ligand with the oxygen

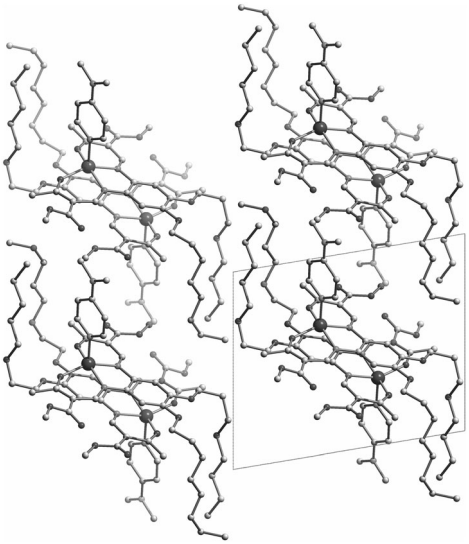

Fig. 6 Molecular packing of **2b** along [100].

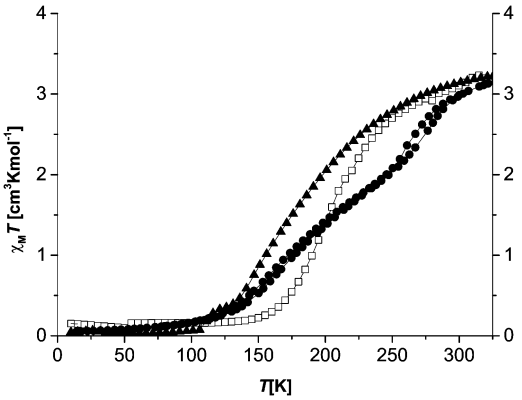

Fig. 7 Magnetic measurement of **1a** (circles), **1b** (triangles) and a methanol solution of **1** with a 50 fold excess of dmap (open squares) in the temperature range of 325–10 K.

atom O4 of the outer periphery of the ligand of the neighbouring molecule. The dmap ligands are arranged parallel to each other and also almost parallel to the alkyl chains. The same is observed for the alkyl chains that are themselves arranged parallel to each other. That means that the alkyl chains of one molecule are again interacting with the chains of another molecule whose axial ligand points to the opposite direction so that they form a lipid layer like arrangement. The distances between the alkyl chains support the idea of stabilising vdW interactions. Additionally, the distances between the stacked planes of the equatorial ligand (about 3.5 Å) suggest stabilising π–π-interactions.

Magnetic measurements

Temperature dependent magnetic measurements in the 325–10 K range were performed for all complexes discussed in this work. Additionally, the temperature dependent magnetic susceptibility was determined in a methanol solution of the iron complex **1** with a 50 fold excess of dmap. The concentration of the complex in the solution is *ca.* 14.5 mg mL^{-1}. The presence of the octahedral complex [Fe(L)(dmap)$_2$] in solution was confirmed by the colour change upon cooling due to the spin transition. This is illustrated in the ESI,† Fig. S4. In Fig. 7 the results for **1a**, **1b** and for the methanol solution of the complex are given. At 325 K **1a** is in the high spin state, with a $\chi_M T$ value of 3.15 cm^3 K mol^{-1}. Upon cooling a gradual decrease of the $\chi_M T$ product down to 2.10 cm^3 K mol^{-1} at 255 K is observed, where a small plateau is visible. Further cooling causes a slow drop of the $\chi_M T$ product until the compound is in the low spin state at about 100 K (0.17 cm^3 K mol^{-1}). The plateau is due to a mixture of powder and crystalline parts in the sample used for the magnetic measurements. According to X-ray structure analysis the crystals contain disordered methanol molecules. Results from CHN analysis indicate the absence of additional methanol molecules in the fine crystalline bulk material. The step and the small hysteresis disappear completely if the compound is measured again after complete removal of the methanol. This is confirmed by a measurement on freshly prepared crystals (**1c**) where in the first cycle an apparent hysteresis is observed (see ESI,† Fig. S3) that is lost in a second cycle. The transition curve of sample **1a** can be reproduced by displaying a combined curve of the weighted contributions (50 : 50) of **1b** and **1c**.

The magnetic properties of **1b** are very similar to that of **1a**. The spin transition is very gradual and complete and takes place in the same temperature region. The $\chi_M T$ value at 325 K is with 3.10 cm^3 K mol^{-1} comparable to that of **1a**. Decreasing of the temperature leads to a gradual decrease of the $\chi_M T$ product until 120 K (0.31 cm^3 K mol^{-1}) where a small plateau can be observed. At 100 K the compound is completely in the LS state ($\chi_M T$ = 0.06 cm^3 K mol^{-1}). Although methanol molecules are included in the crystal packing of **1b**, they are strongly disordered and are, apparently, not involved in cooperative interactions as a very gradual spin transition is observed.

In Fig. S2, ESI,† the spin transition curves of the products of the different synthetic approaches are compared. The penta-coordinated samples (**2a**, **2b** and **2** from the approach with 20 fold excess of dmap) remain as expected in the HS state. The $\chi_M T$ *vs.* *T* plot of **2** is shown as a typical example. All samples, where 50 equivalents of dmap and more was used, show the same kind of spin transition as **1b**, independent of additional solvent or dmap molecules in the crystal packing. This is unexpected as for spin transition compounds often significant changes in the spin transition behaviour are observed, if the crystal packing is slightly modified or additional solvent molecules are included. The behaviour observed for the different samples of **1** indicates the total absence of cooperative interactions, and thus the spin transition should be comparable to that of the complex in solution. As can be seen in Fig. 7, indeed the transition curves are almost identical. Only the transition temperature is shifted to slightly higher temperatures in solution.

It was already shown that abrupt ST is realisable with compounds that bear lipid layer like arrangements.[12] The increase of vdW interactions influences the packing in the crystal through the formation of lipid layer like arrangements and by this cooperative effects like a network of hydrogen

bonds between the polar groups can be enhanced. For the complexes described here, no layered structure can be achieved because of the relatively short C8 alkyl chains. Additionally, the molecule is very bulky and the volume change upon spin transition relative to the overall volume is relatively small and almost in the region of the thermal contraction. Therefore, cooperativity is decreased in the crystal and only a gradual SCO as in solution is observed. This is the reason why the spin transition is independent of the conformation of the molecule and the crystal packing. A similar effect was recently described for the nanostructuring of mononuclear complexes.[19]

Conclusions

In this article, several molecular setups and arrangements of hexa- and penta-coordinated amphiphilic iron(II) complexes **1a** (HS), **1a** (LS), **1b**, **2a** and **2b** with dimethylaminopyridine as axial ligands were investigated with the help of X-ray structure analysis and magnetic measurements. The complex can precipitate hexa-coordinated as well as penta-coordinated depending on the excess of the axial ligand consumed. With 30 equivalents of dmap the system can crystallise in both modifications, below this value it is penta-coordinated and above, it can be forced to crystallise hexa-coordinated. In the case of the octahedral complexes **1a** and **1b**, a gradual spin crossover can be observed starting at about 325 K in the high spin state and ending at about 125 K in the low spin state. It should be pointed out that the spin transition is always the same despite the significant differences in the composition and crystal packing of the different samples. The crystal structures show no lipid layer like arrangement due to the relatively short C8 alkyl chains. In the crystal packing of the penta-coordinated compound vdW interactions between the C8 alkyl chains are observed. This in combination with the π–π-interactions could be the reason for the complex to precipitate penta-coordinated up to a relatively high excess of the used dmap ligand. The gradual spin transition behaviour can be explained with missing lipid layer like arrangement and the absence of other factors that are responsible for cooperative interactions. Thus the same spin transition as in solution is observed.

Experimental section

Synthesis

The synthesis of the iron complexes was carried out under an argon atmosphere using Schlenk tube techniques. The solvents therefore were purified as described in the literature[20] and distilled under an atmosphere of argon. The precursors methoxymethylene-methylacetoacetate,[21] iron(II) acetate,[14] 1,2-dioctyloxybenzene, 1,2-dinitro-4,5-dioctyloxybenzene, 1,2-diamino-4,5-dioctyloxy-benzene[22] were synthesised as described.

(*E*,*E*)[{dimethyl-2,2′[4,5-dioctyloxy-1,2-phenylenebis(iminomethyl-idyne)]bis-3-oxobutanato}] (H_2L). Under argon, 2.1 g (5.76 mmol) of 1,2-diamino-4,5-dioctyloxybenzene and 2.4 g of (15.18 mmol, 2.6 eq.) methoxymethylenemethylacetoacetate were dissolved in 60 mL of degassed ethanol and the yellow solution was heated to reflux for 90 min. After storing the reaction mixture at 5 °C overnight, the precipitate was collected, washed with ethanol and recrystallised from 35 mL of ethanol. The bright yellow fine crystalline ligand was dried in air. Yield: 3.1 g (87%). Elem. anal. calcd for $C_{34}H_{52}N_2O_8$ (616.79 g mol^{-1}): C 66.21, H 8.50, N 4.54; found: C 66.64, H 9.28, N 4.64. MS (DEI+): *m*/*z* (%) = 616 (100) $[M]^+$, 584 (62), 552 (61) 501 (54). ^{1}H NMR (299.86 MHz, $CDCl_3$, 298 K): δ = 0.90 (t, J = 6.8 Hz, 6H, CH_3), 1.30–1.40 (m, 16H, CH_2), 1.45–1.55 (m, 4H, CH_2), 1.80–1.89 (m, 4H, CH_2), 2.57 (s, 6H, CH_3), 3.79 (s, 6H, CH_3), 4.03 (t, 4H, J = 6.5 Hz, CH_2O), 6.76 (s, 2H, H_{ar}), 8.28 (d, 2H, J = 12.5 Hz, CH═), 12.90 (d, 2H, J = 12.5 Hz, NH) ppm. ^{13}C NMR (75.40 MHz, $CDCl_3$, 298 K): δ = 14.3 (CH_3), 22.9 (CH_2), 26.2 (CH_2), 29.4 (CH_2), 29.5 (CH_2), 29.6 (CH_2) 31.3 (CH_3), 32.1 (CH_2), 45.0 (C_q), 51.5 (CH_3), 70.3 (CH_2, CH_2O), 103.7 (C_q), 106.7 (CH, C_{ar}), 125.0 (C_q, C_{ar}–N), 148.8 (C_q, C_{ar}–O), 154.3 (CH), 167.4 (O–C═O), 200.4 (C═O) ppm. IR: $\tilde{\nu}$ = 1699 s, 1612 vs, 1521 m, 1420 m, 1243 vs, 1189 vs, 1081 vs.

[Fe(L)(MeOH)$_2$]. 1.5 g (2.43 mmol) of **H_2L** and 0.85 g of (4.86 mmol, 2 eq.) iron(II) acetate were dissolved in 100 mL of methanol and the brown solution was heated to reflux for 1 h. After cooling to room temperature, the brown precipitate was collected, washed twice with 10 mL of methanol and dried in vacuum. Yield: 1.35 g (76%). Elem. anal. calcd for $C_{36}H_{58}FeN_2O_{10}$ (734.80 g mol^{-1}): C 58.85, H 7.96, N 3.81; found: C 59.29, H 7.86, N 4.16. IR: $\tilde{\nu}$ = 2925 m, 2854 w, 1706 m, 1577 s, 1506 w, 1429 s, 1384 s, 1258 vs, 1214 s, 1069 vs, 998 m, 841 m, 769 m.

[Fe(L)(dmap)$_2$] (1/1a). 0.27 g (0.37 mmol) of [**Fe(L)(MeOH)$_2$**] and 1.35 g of (11.05 mmol, 30 eq.) dmap were dissolved in 15 mL of methanol and heated to reflux for 70 min. After storing the solution at 5 °C for 14 d, greenish-black crystals (**1a**) were filtered and dried in vacuum. Yield: 0.01 g (3%, crystals), 0.15 g (44%, fine crystalline powder, **1**/**1a**) Elem. anal. calcd for $C_{48}H_{70}FeN_6O_8$ (fine crystalline powder, no methanol included) (914.95 g mol^{-1}): C 63.01, H 7.71, N 9.19; found: C 62.67, H 7.78, N 9.59.

[Fe(L)(dmap)] (2a). 0.25 g of (0.34 mmol) [**Fe(L)(MeOH)$_2$**] and 1.25 g of (10.21 mmol, 30 eq.) dmap were dissolved in 10 mL of methanol and heated to reflux for 60 min. After 1 d at room temperature the reaction mixture was stored at −30 °C for 3 d. Black crystals that precipitated were filtered, washed with 2.5 mL of methanol and dried in vacuum. Yield: 0.13 g (48%). Elem. anal. calcd for $C_{41}H_{60}FeN_4O_8$ (792.78 g mol^{-1}): C 62.12, H 7.63, N 7.07; found: C 61.79, H 7.44, N 7.30.

[Fe(L)(dmap)] (2b). 0.18 g (0.25 mmol) of [**Fe(L)(MeOH)$_2$**] and 0.90 g of (7.37 mmol, 30 eq.) dmap were dissolved in 15 mL of methanol and heated to reflux for 60 min. After 5 weeks at room temperature, black needles that precipitated were filtrated and dried in vacuum. Yield: 0.05 g (22%). $C_{41}H_{60}FeN_4O_8$ (792.78 g mol^{-1}). Elem. anal. was not possible due to the insufficient amount of product. IR: $\tilde{\nu}$ = 2923 m, 2853 w, 1693 m, 1579 s, 1433 s, 1387 s, 1255 vs, 1212 vs, 1065 vs, 1008 s, 804 m, 768 m.

[Fe(L)(dmap)]. (20 eq.) 0.25 g (0.34 mmol) of [**Fe(L)(MeOH)$_2$**] and 0.83 g of (6.8 mmol, 20 eq.) dmap were dissolved in 15 mL of methanol and heated to reflux for 60 min. After 1 d at room temperature, black crystals and brown powder were filtered and dried in vacuum. Yield: 0.12 g (44%). Elem. anal. calcd for $C_{41}H_{60}FeN_4O_8$ (792.78 g mol^{-1}): C 62.12, H 7.63, N 7.07; found: C 61.80, H 7.81, N 7.21.

[Fe(L)(dmap)$_2$]. (30 eq.) 0.25 g of (0.34 mmol) [**Fe(L)(MeOH)$_2$**] and 1.25 g (10.2 mmol, 30 eq.) of dmap were dissolved in 15 mL of methanol and heated to reflux for 60 min. After 1 d at room temperature and 10 d at 6 °C, black crystals and brown powder were filtered and dried in vacuum. Yield: 0.16 g (51%). Elem. anal. calcd for $C_{48}H_{70}FeN_6O_8$ (914.95 g mol^{-1}): C 63.01, H 7.71, N 9.19; found: C 62.77, H 8.15, N 9.30.

[Fe(L)(dmap)$_2$] (1b). (50 eq.) 0.27 g of (0.37 mmol) [**Fe(L)(MeOH)$_2$**] and 2.25 g (18.4 mmol, 50 eq.) of dmap were dissolved in 15 mL of methanol and heated to reflux for 70 min. After 1 d at room temperature, 16 d at 6 °C and 1 d at −30 °C, black crystals were filtrated, washed with 3 mL of methanol and dried in vacuum. Yield: 0.05 g (15%). Elem. anal. calcd for $C_{48}H_{70}FeN_6O_8$ (no methanol included) (914.95 g mol^{-1}): C 63.01, H 7.71, N 9.19; found: C 62.87, H 8.03, N 9.66.

[Fe(L)(dmap)$_2$]. (70 eq.) 0.25 g of (0.34 mmol) [**Fe(L)(MeOH)$_2$**] and 2.91 g (23.8 mmol, 70 eq.) of dmap were dissolved in 15 mL of methanol and heated to reflux for 60 min. After 1 d at room temperature, 14 d at 6 °C and 13 d at −30 °C, black crystals were filtrated and dried in vacuum. Yield: 0.15 g (48%). Elem. anal. calcd for $C_{48}H_{70}FeN_6O_8$ × dmap (1037.12 g mol^{-1}): C 63.69, H 7.77, N 10.80; found: C 63.79, H 8.39, N 10.87.

[Fe(L)(dmap)$_2$]. (90 eq.) 0.25 g of (0.34 mmol) [**Fe(L)(MeOH)$_2$**] and 3.74 g (30.6 mmol, 90 eq.) of dmap were dissolved in 15 mL of methanol and heated to reflux for 60 min. After 1 d at room temperature, 14 d at 6 °C and 5 d at −30 °C, black crystals were filtered and dried in vacuum. Yield: 0.16 g (51%). Elem. anal. calcd for $C_{48}H_{70}FeN_6O_8$ × 2dmap × 0.5MeOH (1175.31 g mol^{-1}): C 63.87, H 7.89, N 11.92; found: C 64.06, H 8.24, N 11.68.

[Fe(L)(dmap)$_2$]. (110 eq.) 0.25 g of (0.34 mmol) [**Fe(L)(MeOH)$_2$**] and 4.57 g (37.4 mmol, 110 eq.) of dmap were dissolved in 15 mL of methanol and heated to reflux for 60 min. After 1 d at room temperature, 10 d at 6 °C and 4 d at −30 °C, black fine crystalline powder was filtered and dried in vacuum. Elem. anal. calcd for $C_{48}H_{70}FeN_6O_8$ × 2dmap × 0.5MeOH (1175.31 g mol^{-1}): C 63.87, H 7.89, N 11.92; found C 64.05, H 8.63, N 11.82.

Magnetic measurements

Magnetic measurements on the bulk materials were carried out using a SQUID MPMS-XL5 from Quantum Design with an applied field of 1000, 2000 and 5000 G, respectively, and in the temperature range from 325 to 10 K in the sweep and settle modes. The sample was prepared in a gelatine capsule held in a plastic straw. The raw data were corrected for the diamagnetic part of the sample holder and the diamagnetism of the organic ligand using tabulated Pascal's constants.

For the measurements in solution the sample was prepared in the plastic straw and measured in the settle mode with an applied field of 20 000 G. The raw data were corrected for the diamagnetism of the solution and the diamagnetism of the organic ligand using tabulated Pascal's constants.

X-ray diffraction

The intensity data of **1a** (LS), **1a** (HS), **1b**, **2a** and **2b** were collected using a Stoe IPDS II diffractometer using graphite-monochromated Mo-K$_\alpha$ radiation. The data were corrected for Lorentz and polarisation effects. **1a** (LS) **1b**, **2a** and **2b** (Sir97),[23] **1a** (HS) (SHELXS-97)[24] were solved by direct methods and refined by full-matrix least-squares techniques against F_0^2 (SHELXL-97).[24] The hydrogen atoms were included at calculated positions with fixed displacement parameters, allowed to ride on their parent atoms. If not noted differently, for methyl groups and hydroxyl groups the torsion angles were allowed to be refined according to the electron density. For the hydroxyl groups O99–H9A (**1a**), O98–H98 and O99–H99 (both **1b**) no stable refinement was achieved thus idealised torsion angles were used. All non-hydrogen atoms were refined anisotropically. Due to bad quality of the data of **1b** (bad R_{int}) and **2a** only the general molecular setup could be investigated. For **2a**, twin refinement was conducted based on the twin law

$$\begin{pmatrix} -1.000 & 0.000 & 0.000 \\ 0.000 & -1.000 & 0.000 \\ 0.369 & 0.000 & 1.000 \end{pmatrix}$$

found by PLATON.[25] ORTEP-III[26] was used for the structure representation, Schakal-99[27] and Mercury[28] for the representation of the molecule packing.

Acknowledgements

We thank C. Lochenie, P. Thoma and J. Obenauf (University of Bayreuth) for the collection of the X-ray data and W. Milius for professional support. For financial support we thank the University of Bayreuth and the Deutsche Forschungsgemeinschaft (SFB 840/A10).

Notes and references

1 L. Cambi and L. Szegö, *Ber. Dtsch. Chem. Ges. A/B*, 1933, **66**, 656–661.
2 *Spin-Crossover Materials*, ed. M. A. Halcrow, John Wiley & Sons Ltd, Oxford, UK, 2013.
3 *Spin Crossover in Transition Metal Compounds I-III*, ed. P. Gütlich and H. Goodwin, Springer Berlin/Heidelberg, 2004, pp. 233–235.
4 (*a*) S. Hayami, Y. Komatsu, T. Shimizu, H. Kamihata and Y. H. Lee, *Coord. Chem. Rev.*, 2011, **255**, 1981–1990; (*b*) C. Gandolfi, T. Cotting, P. N. Martinho, O. Sereda, A. Neels, G. G. Morgan and M. Albrecht, *Dalton Trans.*, 2011, **40**, 1855–1865; (*c*) P. N. Martinho, C. J. Harding, H. Müller-Bunz, M. Albrecht and G. G. Morgan, *Eur. J. Inorg. Chem.*, 2010, 675–679; (*d*) Y. Komatsu, K. Kato, Y. Yamamoto, H. Kamihata, Y. H. Lee, A. Fuyuhiro, S. Kawata and S. Hayami, *Eur. J. Inorg. Chem.*, 2012, 2769–2775; (*e*) Y. Bodenthin, U. Pietsch, H. Möhwald and D. G. Kurth, *J. Am. Chem. Soc.*, 2005, **127**, 3110–3114; (*f*) A. B. Gaspar, M. Seredyuk and P. Gütlich, *Coord. Chem. Rev.*, 2009, **253**, 2399–2413.

5 P. Grondin, O. Roubeau, M. Castro, H. Saadaoui, A. Colin and R. Clérac, *Langmuir*, 2010, **26**, 5184–5195.
6 A. Gaspar, M. Seredyuk and P. Gütlich, *J. Mol. Struct.*, 2009, **924–926**, 9–19.
7 (*a*) S. M. Neville, C. Etrillard, S. Asthana and J.-F. Létard, *Eur. J. Inorg. Chem.*, 2010, 282–288; (*b*) V. Martínez, I. Boldog, A. B. Gaspar, V. Ksenofontov, A. Bhattacharjee, P. Gütlich and J. A. Real, *Chem. Mater.*, 2010, **22**, 4271–4281; (*c*) J. R. Galán-Mascarós, E. Coronado, A. Forment-Aliaga, M. Monrabal-Capilla, E. Pinilla-Cienfuegos and M. Ceolin, *Inorg. Chem.*, 2010, **49**, 5706–5714.
8 (*a*) C. Thibault, G. Molnár, L. Salmon, A. Bousseksou and C. Vieu, *Langmuir*, 2010, **26**, 1557–1560; (*b*) M. Cavallini, I. Bergenti, S. Milita, G. Ruani, I. Salitros, Z.-R. Qu, R. Chandrasekar and M. Ruben, *Angew. Chem.*, 2008, **120**, 8724–8728; (*c*) C. M. Quintero, I. A. Gural'skiy, L. Salmon, G. Molnar, C. Bergaud and A. Bousseksou, *J. Mater. Chem.*, 2012, **22**, 3745–3751; (*d*) A. D. Naik, L. Stappers, J. Snauwaert, J. Fransaer and Y. Garcia, *Small*, 2010, **6**, 2842–2846.
9 (*a*) B. Weber, W. Bauer, T. Pfaffeneder, M. M. Dîrtu, A. D. Naik, A. Rotaru and Y. Garcia, *Eur. J. Inorg. Chem.*, 2011, 3193–3206; (*b*) B. Weber, W. Bauer and J. Obel, *Angew. Chem., Int. Ed.*, 2008, **47**, 10098–10101.
10 (*a*) M. Seredyuk, A. B. Gaspar, V. Ksenofontov, Y. Galyametdinov, J. Kusz and P. Gütlich, *J. Am. Chem. Soc.*, 2008, **130**, 1431–1439; (*b*) M. Seredyuk, A. B. Gaspar, V. Ksenofontov, Y. Galyametdinov, J. Kusz and P. Gütlich, *Adv. Funct. Mater.*, 2008, **18**, 2089–2101.
11 S. Schlamp, P. Thoma, B. Weber and Y. Garcia, *Eur. J. Inorg. Chem.*, 2012, 2759–2768.
12 S. Schlamp, B. Weber, A. D. Naik and Y. Garcia, *Chem. Commun.*, 2011, **47**, 7152–7154.
13 S. Hayami, Y. Kojima, D. Urakami, K. Ohta and K. Inoue, *Polyhedron*, 2009, **28**, 2053–2057.
14 B. Weber, R. Betz, W. Bauer and S. Schlamp, *Z. Anorg. Allg. Chem.*, 2011, **637**, 102–107.
15 B. Weber, *Coord. Chem. Rev.*, 2009, **253**, 2432–2449.
16 B. Weber and E.-G. Jäger, *Eur. J. Inorg. Chem.*, 2009, 465–477.
17 S. Schlamp, J. Schulten, R. Betz, T. Bauch, A. V. Mudring and B. Weber, *Z. Anorg. Allg. Chem.*, 2012, **638**, 1093–1102.
18 (*a*) B. Weber, E. Kaps, J. Weigand, C. Carbonera, J.-F. Létard, K. Achterhold and F. G. Parak, *Inorg. Chem.*, 2008, **47**, 487–496; (*b*) B. Weber, J. Obel, D. Henner-Vasquez and W. Bauer, *Eur. J. Inorg. Chem.*, 2009, 5527–5534.
19 A. Tissot, L. Rechignat, A. Bousseksou and M.-L. Boillot, *J. Mater. Chem.*, 2012, **22**, 3411.
20 H. G. O. Becker, *Organikum. Organisch-chemisches Grundpraktikum*, Johann Ambrosius Barth, Berlin, 19th edn, 1993.
21 W. Bauer, T. Ossiander and B. Weber, *Z. Naturforsch., B: Chem. Sci.*, 2010, 323–328.
22 (*a*) M. J. Howard, F. R. Heirtzler and S. I. G. Dias, *J. Org. Chem.*, 2008, **73**, 2548–2553; (*b*) W. M. Lauer, C. Rondestvedt, R. T. Arnold, N. L. Drake, J. van Hook and J. Tinker, *J. Am. Chem. Soc.*, 1946, **68**, 1546–1548; (*c*) M. Schlögl and B. Rieger, *Z. Naturforsch., B: Chem. Sci.*, 2004, 233–240; (*d*) K. Tahara, S. Furukawa, H. Uji-i, T. Uchino, T. Ichikawa, J. Zhang, W. Mamdouh, M. Sonoda, F. C. de Schryver, S. de Feyter and Y. Tobe, *J. Am. Chem. Soc.*, 2006, **128**, 16613–16625.
23 A. Altomare, M. C. Burla, M. Camalli, G. L. Cascarano, C. Giacovazzo, A. Guagliardi, A. G. G. Moliterni, G. Polidori and R. Spagna, *J. Appl. Crystallogr.*, 1999, **32**, 115–119.
24 G. Sheldrick, *Acta Crystallogr., Sect. A: Fundam. Crystallogr.*, 2008, **64**, 112–122.
25 A. L. Spek, *PLATON - A Multipurpose Crystallographic Tool*, Utrecht University, Utrecht, The Netherlands, 2008.
26 (*a*) C. K. Johnson and M. N. Burnett, *ORTEP-III*, Oak-Ridge National Laboratory, Oak-Ridge, TN, 1996; (*b*) L. Farrugia, *J. Appl. Crystallogr.*, 1997, **30**, 565.
27 E. Keller, *Schakal-99*, University of Freiburg, Germany, 1999.
28 C. F. Macrae, P. R. Edgington, P. McCabe, E. Pidcock, G. P. Shilds, R. Taylor, M. Towler and J. van de Streek, *J. Appl. Crystallogr.*, 2006, **39**, 453–457.

